JOURNAL OF SPACECRAFT AND ROCKETS
Vol. 48, No. 3, May–June 2011

Effect of Freestream Noise on Roughness-Induced Transition for a Slender Cone

Katya M. Casper*
Purdue University, West Lafayette, Indiana 47907-1282
Heath B. Johnson†
University of Minnesota, Minneapolis, Minnesota 55455
and
Steven P. Schneider‡
Purdue University, West Lafayette, Indiana 47907-1282

DOI: 10.2514/1.48300

The effect of freestream noise on roughness-induced transition was studied on a blunt 7 deg half-angle cone in the Boeing and U.S. Air Force Office of Scientific Research Mach-6 Quiet Tunnel. Temperature-sensitive paints were used to visualize the wake of an isolated roughness element at 0 and 6 deg angles of attack. Transition onset was determined from the rise in centerline temperature downstream of the roughness. Transition was always delayed under quiet flow compared with noisy flow. For example, at 0 deg angle of attack, transition was up to 6.3 times further downstream from the trip location. The difference in transition location between quiet and noisy flow conditions was significantly reduced when an effective trip height was reached. However, quiet flow still delayed transition by a factor of 2.4 in those cases. Because quiet flow delays transition behind a roughness element, the height of trips sized in a conventional noisy tunnel should be increased for quiet flightlike conditions. On the other hand, any naturally occurring roughness that causes transition under noisy flow might not cause transition in a quiet environment.

Nomenclature

AOA	=	angle of attack, deg
k	=	roughness height, mm
L	=	model length, mm
M	=	freestream Mach number
P_0	=	tunnel stagnation pressure, kPa
T_0	=	tunnel stagnation temperature, K
t	=	time into run, s
Re/m	=	freestream unit Reynolds number, 1/m
Re_k	=	Reynolds number based on roughness height k and local conditions in the undisturbed boundary layer at the height k
x_k	=	axial location of roughness, mm
x_{tr}	=	axial location of transition onset, mm
y^+	=	distance from the wall normalized by the viscous lengthscale
δ^*	=	boundary-layer displacement thickness, mm

I. Introduction

LAMINAR–TURBULENT transition is important for reentry vehicles since it affects parameters such as heat transfer and skin friction. These affect the thermal protection system, the glide distance for long-range hypersonic vehicles, and other design considerations. However, transition can be difficult to predict. One factor affecting transition is surface roughness, whether it is an intentional part of the vehicle design or an artifact of the vehicle's construction. Understanding the effect of roughness on transition and being able to predict where transition will occur when roughness is present is a major thrust of current hypersonic research.

Many studies have been conducted on roughness effects. Schneider [1] reviewed roughness-induced transition, stating "the effect of roughness on hypersonic boundary-layer transition has been studied for three primary purposes: to trip a laminar layer to turbulence, to determine whether naturally occurring roughness is expected to cause early transition, and to determine the largest allowable roughness that will not affect the location of transition." Therefore, depending on the application, roughness can be thought of as either a roughness element or a boundary-layer trip.

Most research on roughness-induced transition has been conducted in conventional tunnels. The noise levels in these tunnels, defined as the root-mean-square pitot pressure divided by the mean pitot pressure, is typically near 1% and sometimes as high as 2–5% [2]. These conventional tunnel noise levels are an order of magnitude higher than flight [3,4]. High noise levels have been shown to cause transition on models much earlier than in flight [3–5]; however, only a few studies have looked at the effect of noise on roughness-induced transition [6–9]. Several of these studies have been conducted in the Boeing and U.S. Air Force Office of Scientific Research (AFOSR) Mach-6 Quiet Tunnel (BAM6QT). The BAM6QT is one of two operational hypersonic quiet tunnels in the world. It features low noise of about 0.05%, which is similar to flight and an order of magnitude lower than conventional tunnels [10]. This makes the tunnel unique for studying transition.

A series of flight tests aimed at developing a better understanding of roughness-induced transition is being conducted under the Hypersonic International Flight Research and Experimentation (HIFiRE) project [11]. The first flight studied natural transition on a slender cone and boundary-layer transition behind a roughness element. Successful flight of the vehicle occurred on 22 March 2010. To properly size the roughness element so that it would cause transition on the vehicle, wind-tunnel tests of the HIFiRE-1 vehicle near flight conditions were conducted at Calspan–University at Buffalo Research Center [12] and also at NASA Langley Research Center (NASA LaRC) [13]. One of the purposes of the BAM6QT

Presented as Paper 2008-4291 at the 38th Fluid Dynamics Conference and Exhibit, Seattle, WA, 23–26 June 2008; received 12 May 2010; revision received 21 September 2010; accepted for publication 21 January 2011.

*Research Assistant, School of Aeronautics and Astronautics. Student Member AIAA.
†Senior Research Associate, Department of Aerospace Engineering and Mechanics. Senior Member AIAA.
‡Professor, School of Aeronautics and Astronautics. Associate Fellow AIAA.

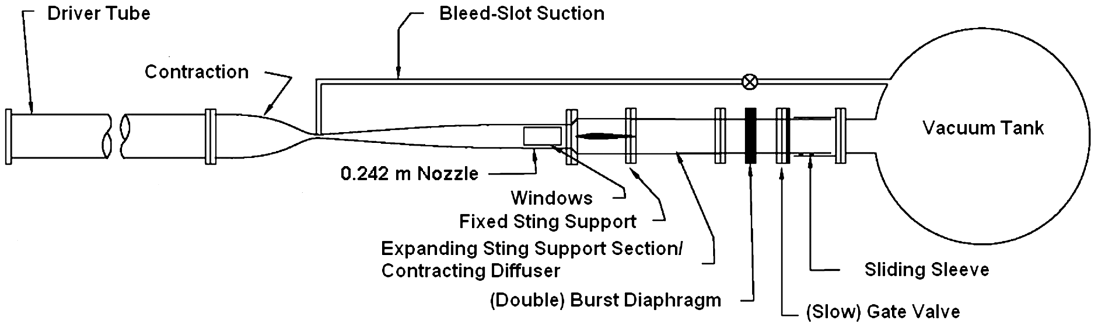

Fig. 1 Boeing/AFOSR Mach-6 Quiet Tunnel.

tests was to show the effect of noise on those measurements. This was to help ensure that a roughness element designed using conventional wind tunnels was sized properly to ensure transition under quiet flight conditions. A parametric study of roughness-height effects on transition was also conducted in the BAM6QT under quiet and noisy conditions. This was used to study the effect of noise on roughness-induced transition for a wider range of applications, whether it involves tripping a boundary layer to turbulence, or determining if transition will occur behind any roughness on a flight vehicle.

II. Boeing/AFOSR Mach-6 Quiet Tunnel

The BAM6QT (Fig. 1) can be operated as a conventional noisy tunnel or as a quiet tunnel. The tunnel is a Ludwieg tube: a long tube with a converging–diverging nozzle on the end. Flow is initiated by bursting a double diaphragm that is located downstream of the diffuser. When the flow begins, an expansion wave travels upstream and then reflects between the upstream end of the driver tube and the contraction. The total pressure and temperature drop with each reflection cycle (every 200 ms) until the tunnel unstarts. Run times of 3–5 s are typical at present. The tunnel uses air as the test gas and operates with an initial total pressure P_0 of 34–2070 kPa and an initial total temperature T_0 of 430 K, giving a freestream unit Reynolds number (Re/m) range of 0.4–18.3 $\times$ 10^6, calculated using Keyes's law for viscosity [14]. The current maximum quiet stagnation pressure is 1130 kPa. The test-section diameter is 0.242 m at the nozzle exit, and the nozzle is 2.590 m long. Noise levels vary from 2–4.5% under noisy flow conditions. Under quiet flow conditions, noise levels are approximately 0.05% [10].

Obtaining quiet flow in a hypersonic tunnel is not a trivial task. The nozzle is polished to a mirror finish to avoid roughness-induced transition, and the contraction boundary layer is also removed by bleed slots at the throat. A new laminar boundary layer then begins just upstream of the nozzle throat and is maintained through the test section. In addition, the air is filtered to remove dust or other particles above 0.01 μm that may damage the nozzle or trip the boundary layer. More details about the development of the BAM6QT can be found in [15].

III. Wind-Tunnel Model and Roughness Elements

The model used in the current experiments was a 7 deg half-angle nylon cone with a 102 mm base diameter. This slender cone represented a 36.9%-scale model of the fore cone of the HIFiRE-1 vehicle, with the exception of the nose, which was stainless steel with a nose radius of 1.19 mm. This radius was chosen to match the size of the full-vehicle models tested at NASA LaRC. The nylon portion of the cone stretches axially from 147 to 405 mm. This portion of the cone was part of an existing model, so the joint between the nylon cone and the nosetip was predefined. Reference marks were applied for image alignment on the nylon frustrum.

The nylon section of the cone was painted with temperature-sensitive paint (TSP). The TSP provides a surface temperature distribution that is used to visualize the wake behind the roughness elements. The TSP is only qualitative for heat transfer at this time; the surface temperature is monotonic in the heat transfer. Work to reduce uncertainty in the measurement and subsequent heat transfer calculations is ongoing [16]. The layer of TSP creates a forward-facing step of about 0.04 mm at the junction between the nosetip and the nylon portion of the cone. The nylon acts as an insulator, which increases the temperature variations seen at the surface. The TSP consisted of Ru(bpy) luminophore molecules in clear automotive paint. The paint was excited during a run with 464 nm light from a 102-mm-diam ISSI LM4 blue light-emitting-diode array. A calibration was conducted to relate the measured intensity ratio of the flow-off and flow-on photographs to the model surface temperature. A 12-bit Photometrics SensysB cooled charge-coupled-device camera was used to capture the images.

A single roughness element was placed on the model for each run as shown in Fig. 2. Roughness elements were 1.27 by 1.27 mm squares, sized to match NASA LaRC's wind-tunnel-test trips. The trips were made from plastic shims and glued to the model. Each trip was placed with a corner in line with the freestream. The trip was placed at an axial distance of 130 mm ($x/L = 0.32$) to equal the trip Reynolds number Re_k for NASA LaRC at the BAM6QT maximum quiet pressure of 931 kPa. For all measurements at angle of attack, the trip was on the windward ray.

A number of parameters were varied during testing. The model was run at 0 and 6 deg angles of attack. The trip height was varied between 0.10 and 0.71 mm. Most tests were run starting at an initial stagnation temperature of 433 K and at the maximum quiet pressure of the tunnel. The freestream unit Reynolds number range of the pictures analyzed was between 8.7–10.0 $\times$ 10^6 /m. Noise levels are near 2.5% at these conditions under noisy flow.

IV. Data Analysis

Trip effectiveness, transition location, and noise effects were studied using the TSP images. Figure 3 shows a typical example of the temperature data. Transition onset is inferred from centerline temperature traces behind the roughness elements, when the temperature begins to rise. This is typically before the wake behind the trip starts to spread. Consider the first trace shown in Fig. 3b. The flow is laminar at the beginning of the trace. The temperature is low and has a small negative slope. This temperature decrease is due to a

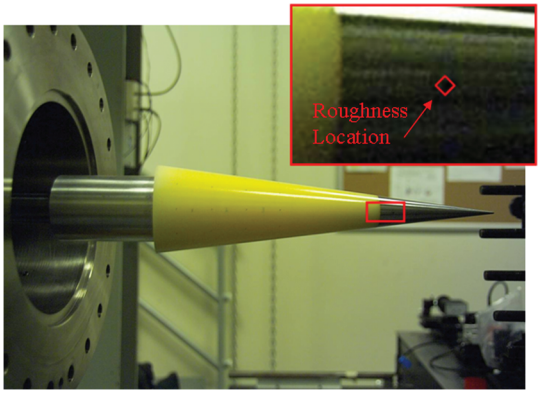

Fig. 2 Model setup for testing in the BAM6QT.

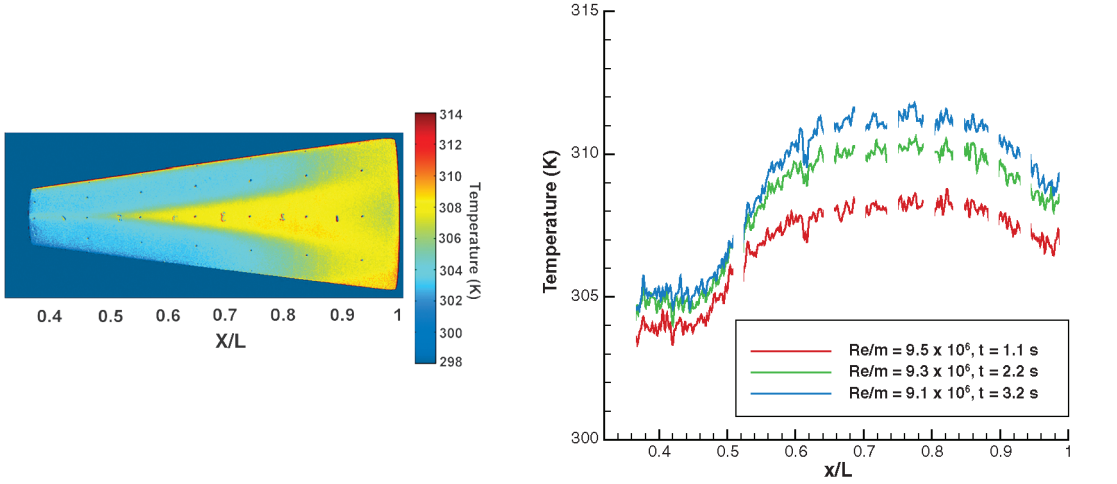

a) TSP image showing boundary-layer transition at $Re/m = 9.1 \times 10^6$

b) Centerline surface-temperature distribution. The freestream unit Reynolds number drops as the run progresses

Fig. 3 Boundary-layer transition downstream of a 0.36 mm trip (noisy flow at 0 deg AOA).

slow, streamwise decrease in heat transfer associated with the gradual thickening of the boundary layer along the model surface. A sharp rise in surface temperature is seen during transition, and the temperature levels off again near the end of transition. The remainder of the temperature trace has a small downward slope, which is due to the growth of the now turbulent boundary layer. It should be noted that the BAM6QT has curved windows that conform to the interior of the nozzle. The axial location of transition is not altered by the curved windows, but the radial extent of the cone changes slightly. This radial distortion has not been corrected, as it does not interfere with comparing noisy and quiet effects or distort the transition location.

Because of the use of an imperfectly insulating model, the mean surface temperature of the model increases during the run, making it difficult to compare pictures taken at significantly different times during the run. Images are compared between noisy and quiet flow at similar times during the run. This means that P_0 and T_0 are similar; however, because the freestream Mach number changes from 5.8 to 6.0 between noisy and quiet flow runs, the freestream unit Reynolds number is approximately 10% lower during quiet flow runs. This Mach number change was not taken into account in the calculations of [17] (the Mach number was always treated as 6.0), but it is here. To see the effect of this unit Reynolds number difference, noisy flow images that better matched unit Reynolds numbers under quiet flow were analyzed. This is done by taking a noisy flow image from later in a run, when both P_0 and T_0 have dropped. Centerline temperature traces during the run were analyzed to see how they would change with time. Figure 3b shows a typical example with a 5% decrease in freestream unit Reynolds number. The change in transition onset location under noisy flow with this Re/m drop is not discernible, although the mean surface temperature increases. Repeat runs were also conducted with small variations in freestream condition and image time. No noticeable change in the results, transition location, or transition footprint were found. Therefore, the comparisons between transition location for quiet and noisy runs were accepted despite the slightly different Re/m.

V. Mean Flow Computations

Navier–Stokes computations provided the boundary-layer edge conditions and the roughness Reynolds numbers that were used to quantify the experimental results. The freestream conditions for the computations were $M = 6.0$, $P_0 = 896$ kPa, and $T_0 = 430$ K. An isothermal wall at 300 K was used for the model temperature. A single-species air model was used.

A. Mean Flow Solutions

For the axisymmetric mean flow solutions, 360×360 point structured grids were generated using STABL [18] with clustering both at the body surface and at the tip of the cone. The outer grid shape was specified to closely follow the shock. The three-dimensional mesh for the cone at angle of attack was generated using GridPro. Clustering of points was applied near the body surface and near the tip of the cone, and grid tailoring was used to closely align the outer surface of the 3-D grid to the shock shape. The 3-D structured multiblock mesh consisted of hexahedral elements and contained approximately 5 million grid cells.

To ensure that the boundary layer solutions were well-resolved, grid point clustering in the body-normal direction was adjusted to obtain values of y^+ less than unity at the first solution point away from the wall. For the axisymmetric case, approximately half the total number of grid points were placed within the boundary layer. For the cone at AOA, approximately 40 grid points were used to resolve the boundary layer.

The laminar mean flow for the axisymmetric solution was generated using an optimized 2-D/axisymmetric mean flow solver based on the implicit Data-Parallel Line Relaxation (DPLR) method [19]. The solver produces second-order-accurate laminar flow solutions with low dissipation and shock capturing. The laminar mean flow solutions for the 3-D tests were generated using the unstructured 3-D implicit solver US3-D, which implements the DPLR and full matrix point relaxation methods [20].

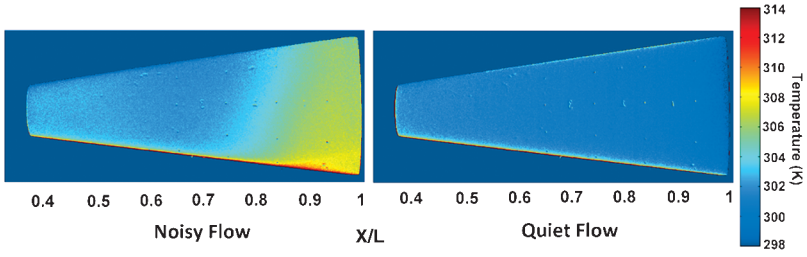

Fig. 4 Natural transition under noisy and quiet flow at 0 deg AOA.

Table 1 Run conditions for natural transition at 0 and 6 deg AOA

AOA, deg	Noisy/quiet	P_0, kPa	T_0, K	t, s	$Re/m \times 10^6$
0	Noisy	961	428	0.97	10.3
0	Quiet	888	427	0.75	8.8
6, side view	Noisy	904	429	0.77	9.6
6, side view	Quiet	891	426	0.80	8.8
6, windward view	Noisy	908	429	0.85	9.7
6, windward view	Quiet	872	425	0.99	8.7

B. Mean Flow Integral and Roughness Calculations

Mean flow integral quantities such as the boundary-layer displacement thickness were calculated using the flow analysis features of STABL. The roughness Reynolds number was calculated as

$$Re_k = \frac{\rho_k u_k k}{\mu_k}$$

where ρ_k, u_k, and μ_k are the local density, velocity, and viscosity in the undisturbed laminar boundary layer at the roughness height k.

VI. Experimental Results

A. Smooth-Wall Transition Under Noisy and Quiet Flow

The model was tested with no roughness to obtain a baseline comparison between quiet and noisy flow. Figure 4 shows the cone at 0 deg angle of attack under both noisy and quiet flow. Run conditions for the images are shown in Table 1. Transition is apparent in the noisy flow case, as indicated by the temperature rise on the aft section of the model. The transition front is approximately 10% asymmetric, possibly due to a small angle of attack on the model, flow non-uniformity, or paint imperfections. Under quiet flow, the boundary layer remains laminar to the end of the model.

A clear difference between noisy and quiet flow is also seen at angle of attack. Figure 5 shows the model at 6 deg AOA with no trip. Run conditions for these images are also listed in Table 1. Under noisy flow, transition begins away from the windward side. Transition then appears to propagate toward the windward ray. Under quiet flow, laminar flow is maintained to the end of the cone. Crossflow vortices are visible under quiet flow, and may be the cause for natural transition under noisy flow at angle of attack. These have also been seen under noisy flow [21] but are not apparent in this case. These results are typical of slender cones studied previously in the BAM6QT.

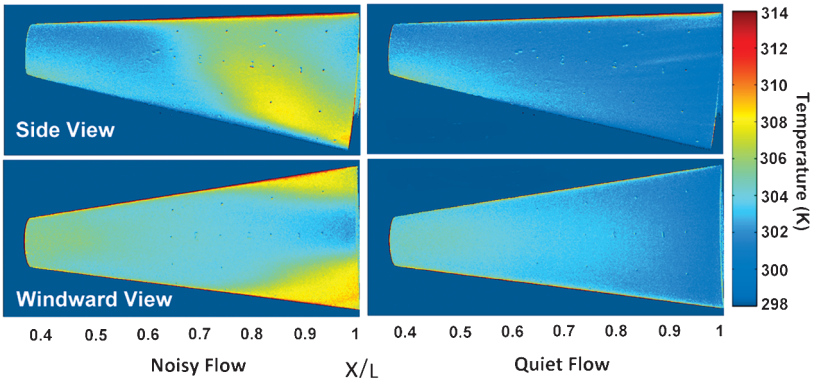

Fig. 5 Natural transition under noisy and quiet flow at 6 deg AOA.

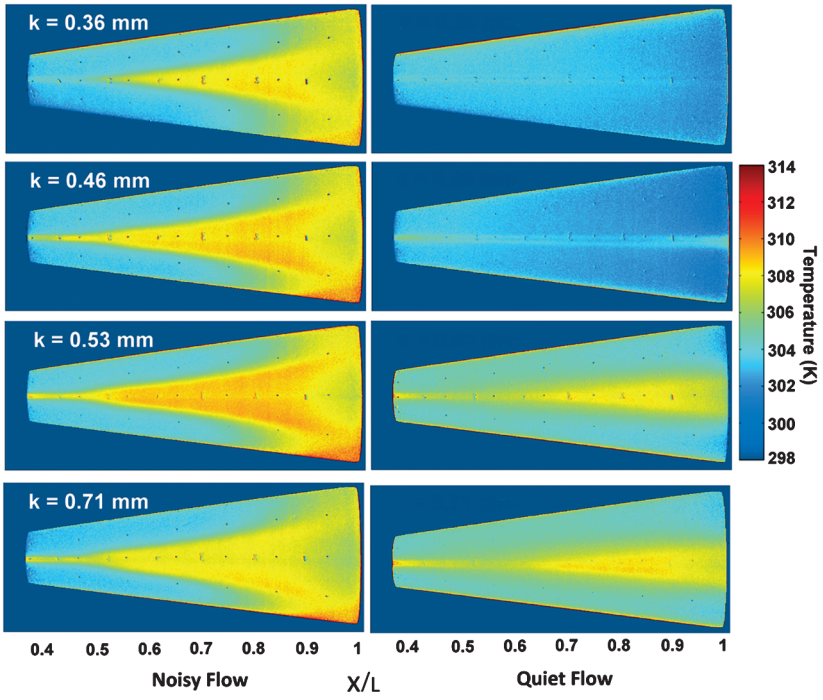

Fig. 6 Effect of trip height under noisy and quiet flow at 0 deg AOA. Trip location is at the left edge of each subfigure ($x/L = 0.32$).

Table 2 Image conditions and transition location for various trip heights at 0 deg AOA

Noisy/quiet	k, mm	P_0, kPa	T_0, K	t, s	$Re/m \times 10^6$	x_{tr}/L
Noisy	0.36	889	427	1.1	9.5	0.46
Noisy	0.46	892	426	1.2	9.6	0.41
Noisy	0.53	885	426	1.3	9.5	0.41
Noisy	0.71	902	427	1.0	9.7	0.41
Quiet	0.36	885	425	0.89	8.8	——
Quiet	0.46	865	423	1.2	8.7	0.87
Quiet	0.53	877	425	1.0	8.7	0.54
Quiet	0.71	873	424	1.1	8.7	0.54

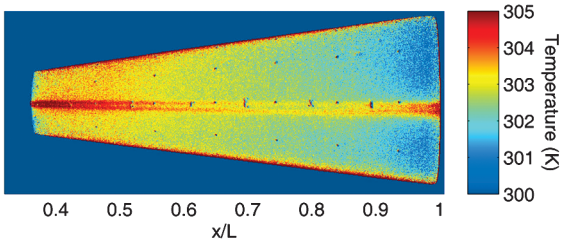

Fig. 8 Rescaled surface temperature plot of $k = 0.46$ mm trip under quiet flow, showing two hot streaks and transition onset well downstream of the roughness.

B. Effect of Trip Height

A parametric study of trip height was conducted with the cone at both 0 and 6 deg angles of attack. Figure 6 shows the model under noisy and quiet flow at 0 deg angle of attack for increasing trip heights from 0.36–0.71 mm. These heights vary from 2.2 to 4.3 times δ^* at the trip location. Flow conditions for each image and the measured transition locations at 0 deg AOA are found in Table 2. In most cases, two straight streaks can be seen in the wake of the roughness element. Downstream of the trip, the wake typically spreads and a turbulent wedge appears. Figure 7 plots the centerline temperature traces for noisy and quiet flow, respectively. Transition onset is inferred when a rise is seen in the centerline surface temperature and is marked by an X on the temperature plots. Some of the trips are large enough to be considered effective. An effective trip is defined as one for which a further increase in height does not cause transition to move further forward.

Under noisy flow, the transition location behind the roughness element does not vary much, for the range of roughness heights tested. The smallest roughness height of 0.36 mm is not fully effective at 0 deg AOA. A further increase in trip height causes transition to move further forward. However, the 0.46 mm trip and the 0.53 and 0.71 mm trips cause transition at approximately the same location on the model. This indicates that the 0.46 mm trip was fully effective under noisy flow. Under quiet flow, the 0.36-mm-high trip generates two hot streaks, but the flow remains laminar to the end of the cone. The 0.46-mm-high trip also generates two streaks in its wake, and transition begins just before the end of the model, as indicated by the centerline temperature trace. The quiet flow image for $k = 0.46$ mm is shown rescaled in Fig. 8 to better show the two streaks downstream of the roughness. The 0.53 and 0.71-mm-high trips both cause transition downstream of the trip, but the transition location does not change significantly between these two trip heights. This indicates that the effective transition height for quiet flow conditions has been reached.

Figure 9 plots the roughness Reynolds number for each trip height against the transition onset location under both noisy and quiet flow. The smallest trip height corresponds to the smallest roughness Reynolds number. A noticeable difference between the noisy and quiet flow conditions can be seen. The same trip heights that cause transition on the model under noisy flow do not necessarily cause transition on the model in quiet flow. When transition does occur, it is delayed. The ratio of transition location under noisy and quiet flow at 0 deg AOA with respect to the trip location can be seen in Table 3. For a less-than-effective trip under quiet flow, there is a significant difference between quiet and noisy flow transition location. For example, for a trip height of 0.46 mm, quiet flow delays transition by

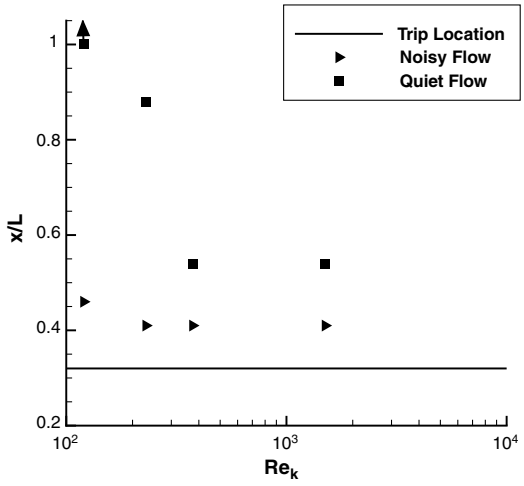

Fig. 9 Effect of trip Reynolds number on transition location at 0 deg AOA.

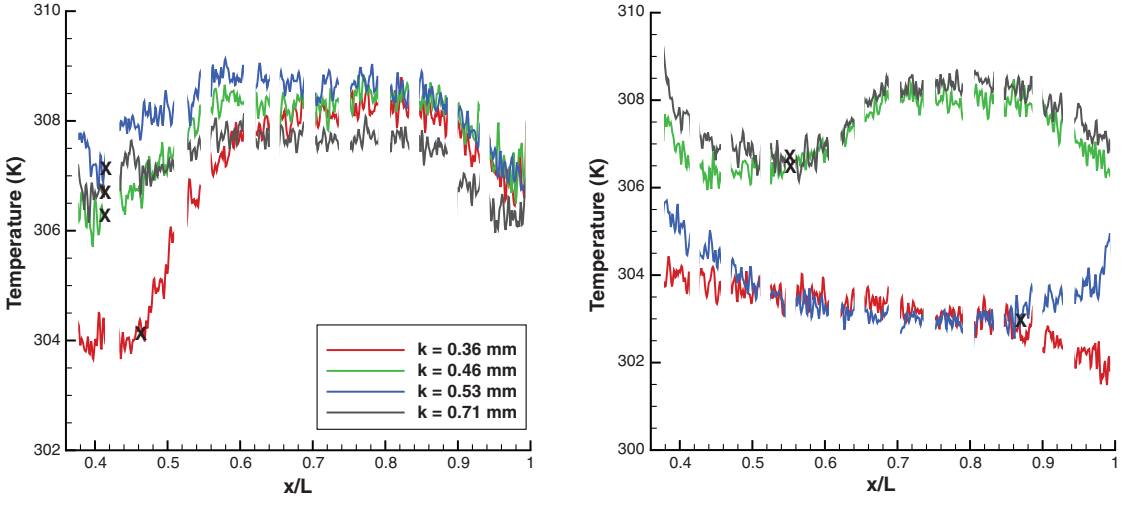

a) Noisy Flow **b) Quiet Flow**

Fig. 7 Centerline temperature distributions at 0 deg AOA. Transition onset is marked by an X.

Table 3 Summary of noise effects on roughness-induced transition at 0 deg AOA

k, mm	k/δ^*	$(x_{tr_{quiet}} - x_k)/(x_{tr_{noisy}} - x_k)$	Flow condition for trip effectiveness
0	0	——	——
0.36	2.2	——	Neither
0.46	2.8	6.3	Noisy
0.53	3.2	2.4	Both
0.71	4.3	2.4	Both

6.3 times, when referenced to the trip location. It had been commonly assumed that tunnel noise would only affect transition location for less-than-effective trips [1,22]. However, a significant delay in the transition location is still observed even with the largest trips, which are effective under quiet flow. For these large trips, transition occurs about 2.4 times farther downstream under quiet flow.

In summary, transition is farther downstream under low-noise flightlike conditions than under high-noise conventional-tunnel conditions at 0 deg AOA. For a less-than-effective trip under flight conditions, the difference in transition location can be significant. For a large trip that is effective under noisy or quiet flow conditions, the

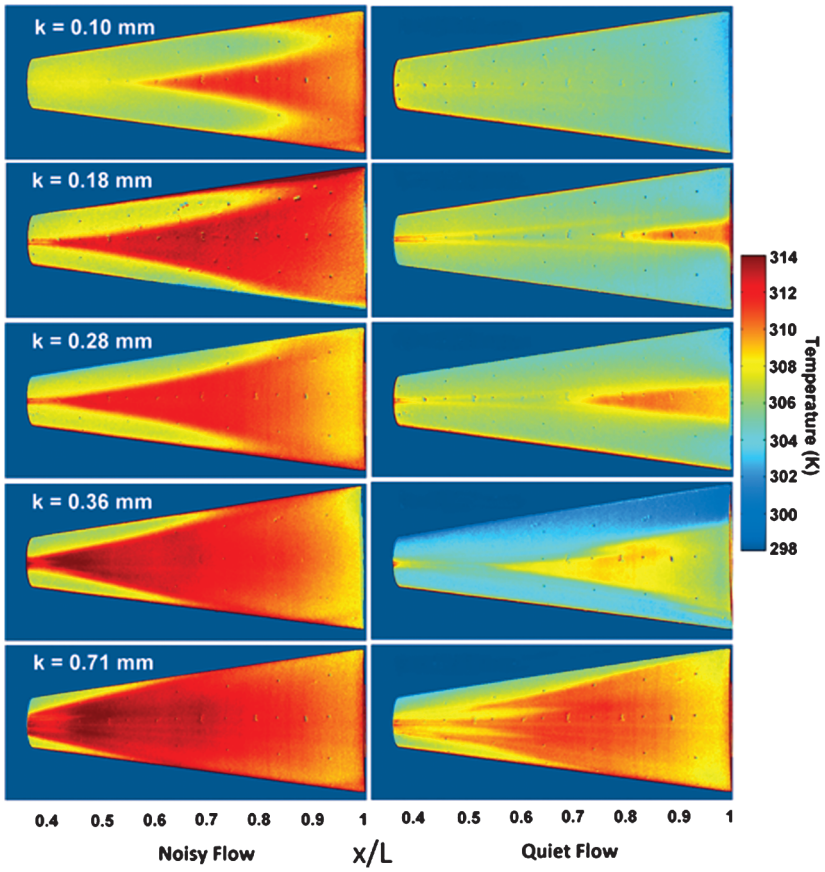

Fig. 10 Effect of trip height under noisy and quiet flow at 6 deg AOA. Trip location is at the left edge of each subfigure ($x/L = 0.32$).

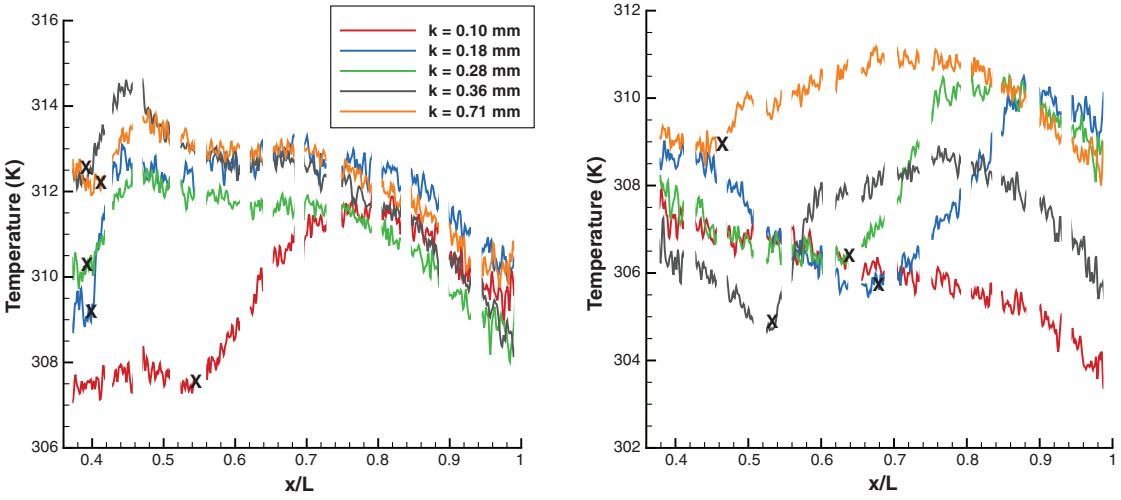

a) Noisy Flow **b) Quiet Flow**

Fig. 11 Centerline temperature distributions at 6 deg AOA. Transition onset is marked by an X.

Table 4 Image conditions and transition location for various trip heights at 6 deg AOA

Noisy/Quiet	k, mm	P_0, kPa	T_0, K	t, s	$Re/m \times 10^6$	x_{tr}/L
Noisy	0.10	905	428	0.89	9.7	0.54
Noisy	0.18	892	427	1.1	9.6	0.40
Noisy	0.28	900	429	0.79	9.6	0.39
Noisy	0.36	938	427	1.0	10.0	0.39
Noisy	0.71	901	427	1.0	9.7	0.41
Quiet	0.10	883	425	0.89	8.8	——
Quiet	0.18	831	418	1.8	8.5	0.68
Quiet	0.28	894	426	0.77	8.8	0.63
Quiet	0.36	897	425	0.91	8.9	0.53
Quiet	0.71	891	426	0.79	8.8	0.45

difference in transition location will be smaller, but still significant. Thus, when sizing a trip for flight using data from a conventional tunnel, the roughness should be made larger. Also, a roughness that causes transition under noisy flow conditions may not cause transition on the vehicle in low-noise flightlike conditions.

C. Angle-of-Attack Effects

The trip height was also varied on the cone at 6 deg AOA. The windward boundary layer is thinner at angle of attack, which makes smaller trip heights more effective. Trip heights ranging from 0.10 to 0.71 mm were tested, which corresponds to trip heights of 1.1 to 7.7 times δ^* at the trip location. Figure 10 shows the resulting surface temperature plots for increasing trip heights under noisy and quiet flow. Figure 11 shows the centerline temperature traces and transition onset locations. Flow conditions for each image and the measured transition locations are found in Table 4.

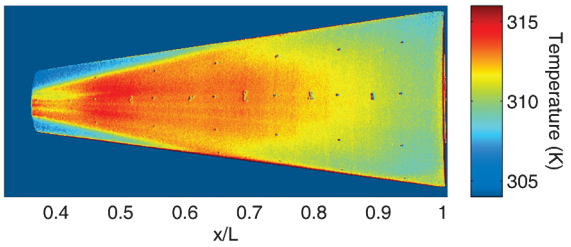

Fig. 12 Rescaled surface temperature plot of $k = 0.71$ mm trip under noisy flow, showing multiple hot streaks and turbulent wedges downstream of roughness.

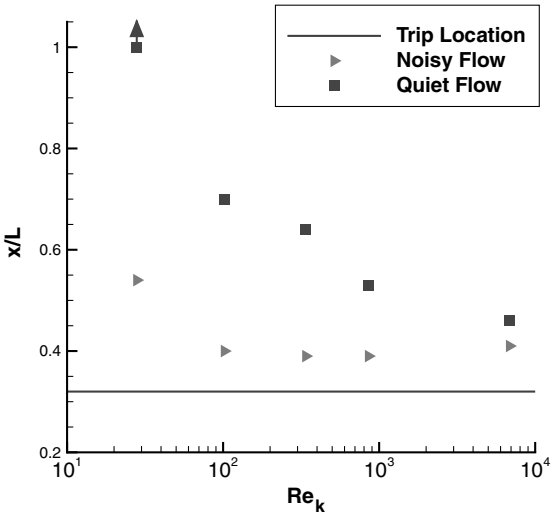

Fig. 13 Effect of trip Reynolds number on transition location at 6 deg AOA.

Table 5 Summary of noise effects on roughness-induced transition at 6 deg AOA

k, mm	k/δ^*	$(x_{tr_{quiet}} - x_k)/(x_{tr_{noisy}} - x_k)$	Flow condition for trip effectiveness
0	0	——	——
0.10	1.1	——	Neither
0.18	1.9	4.4	Noisy
0.28	3	4.4	Noisy
0.36	3.8	3.0	Noisy
0.71	7.7	1.4	Noisy

Under noisy flow, the 0.10 mm trip generates two hot streaks, and transition occurs well downstream of the trip. The 0.18 and 0.28 mm trips both generate two hot streaks. Transition occurs downstream of the trip and remains almost constant between these two trip heights, indicating that a 0.18 mm trip is effective under noisy flow. At the higher trip heights of 0.36 and 0.71 mm, the transition footprint looks different. The temperature behind the roughness element is very high and the wake is much wider. From Fig. 10, it may seem that transition occurs immediately behind the roughness; however, the centerline temperature traces show that transition still occurs downstream of the roughness. A rescaled image shows that there are multiple hot streaks and turbulent wedges downstream of the roughness for the 0.71 mm trip under noisy flow (Fig. 12). The wake is asymmetric, but the top and centerline wedges begin downstream of the front edge of the nylon. The bottom wedge seems to begin upstream of this edge. The combination of the three turbulent wedges makes the transition front much wider. Multiple streaks downstream of a roughness have been noted before behind large roughness [23,24]. The wide wake for large roughness arises from a large region of reversed flow in front of the roughness.

The transitional behavior is similar under quiet flow, though transition is once again delayed when compared with noisy flow. For the shortest trip, neither hot streaks nor transition are seen on the cone. For the 0.18 and 0.28 mm trips, transition occurs but is delayed compared with noisy flow. The two hot streaks generated by the trip curve away from each other in these cases. This spanwise spreading of the streamwise hot streaks indicates outward-directed crossflow. Transition is again delayed at trip heights of 0.36 and 0.71 mm. The transition onset location continues to move forward with increasing trip height, making it unclear whether the 0.71 mm trip is fully effective under quiet flow (Fig. 13). Also, a marked change in the temperature surface plots is again seen at higher trip heights of 0.36 and 0.71 mm. Instead of only two hot streaks, multiple streaks are evident behind the roughness element. Each pair of streaks leads to the formation of a turbulent wedge and transition. As in the noisy flow cases, there is higher heating downstream of the roughness, probably because the trip is oversized.

As before, quiet flow has a marked effect on roughness-induced transition. Transition under quiet flow is delayed as shown in Fig. 13 and in Table 5. However, different trip heights were effective at 0 and 6 deg angles of attack. Under noisy flow at 0 deg angle of attack, a trip height of $k/\delta^* = 2.8$ effectively tripped the flow. At angle of attack, a similar height of $k/\delta^* = 1.9$ was effective. Under quiet flow, there was a much larger difference in effective trip heights with varying angles of attack. At 0 deg AOA, $k/\delta^* = 3.2$ was effective, but at 6 deg, a trip height of $k/\delta^* = 7.7$ was still not fully effective.

VII. Conclusions

Freestream noise was shown to have a significant effect on transition induced by an isolated roughness on a slender cone. Transition behind the roughness element was always delayed under quiet flow. The largest delay was seen for a less-than-effective trip. In that case, transition occurred up to 6.3 times further downstream of the trip. Using effective trip heights reduced the transition delay seen under quiet flow conditions. For example, at 0 deg AOA, transition occurred 2.4 times further downstream when an effective trip was used. However in some cases, roughness that was effective under

conventional noise was not effective under quiet flow. This difference in effective trip height was largest at angle of attack when quiet flow required a much higher roughness to effectively trip the flow. These results shows that a trip sized in a conventional tunnel is not conservative; transition will occur further downstream in low-noise conditions. However, the transition delay seen under quiet flow can be helpful for avoiding unwanted transition downstream of naturally occurring roughness. A larger tolerance for that roughness should exist under quiet flightlike conditions.

Acknowledgments

This work could not have been completed without the help of many individuals. The Ludwieg Tube Group (Matt Borg, Michael Hannon, Tom Juliano, Brad Wheaton, and especially Erick Swanson) provided advice and suggestions throughout the project. Thanks are also extended to Roger Kimmel for help in planning the HIFiRE BAM6QT experiments. This work was funded in part by the National Defense Science and Engineering Graduate Fellowship, Sandia National Laboratories, and the U.S. Air Force Office of Scientific Research.

References

[1] Schneider, S. P., "Effects of Roughness on Hypersonic Boundary-Layer Transition," *Journal of Spacecraft and Rockets*, Vol. 45, No. 2, March–April 2008, pp. 193–209. doi:10.2514/1.29713

[2] Laderman, A. J., "Review of Wind-Tunnel Freestream Pressure Fluctuations," *AIAA Journal*, Vol. 15, No. 4, 1977, pp. 605–608. doi:10.2514/3.7353

[3] Beckwith, I. E., and Miller, C. G. III., "Aerothermodynamics and Transition in High-Speed Wind Tunnels at NASA Langley," *Annual Review of Fluid Mechanics*, Vol. 22, 1990, pp. 419–439. doi:10.1146/annurev.fl.22.010190.002223

[4] Schneider, S. P., "Effects of High-Speed Tunnel Noise on Laminar-Turbulent Transition," *Journal of Spacecraft and Rockets*, Vol. 38, No. 3, 2001, pp. 323–333. doi:10.2514/2.3705

[5] Schneider, S. P., "Flight Data for Boundary-Layer Transition at Hypersonic and Supersonic Speeds," *Journal of Spacecraft and Rockets*, Vol. 36, No. 1, 1999, pp. 8–20. doi:10.2514/2.3428

[6] Borg, M. P., and Schneider, S. P., "Effect of Freestream Noise on Roughness-Induced Transition for the X-51A Forebody," *Journal of Spacecraft and Rockets*, Vol. 45, No. 6, Jan. 2008, pp. 1106–1116. doi:10.2514/1.38005

[7] Creel, T., Beckwith, I., and Chen, F., "Transition on Swept Leading Edges at Mach 3.5," *Journal of Aircraft*, Vol. 24, No. 10, Oct. 1987, pp. 710–717. doi:10.2514/3.45511

[8] Ito, T., Randall, L. A., and Schneider, S. P., "Effect of Noise on Roughness-Induced Boundary-Layer Transition for Scramjet Inlet," *Journal of Spacecraft and Rockets*, Vol. 38, No. 5, 2001, pp. 692–698. doi:10.2514/2.3754

[9] Kegerise, M. A., Owens, L. R., and King, R. A., "High-Speed Boundary-Layer Transition Induced by an Isolated Roughness Element," AIAA Paper 2010-4999, June 2010.

[10] Juliano, T., Schneider, S., Aradrag, S., and Knight, D., "Quiet-Flow Ludwieg Tube for Hypersonic Transition Research," *AIAA Journal*, Vol. 46, No. 7, 2008, pp. 1757–1763. doi:10.2514/1.34640

[11] Kimmel, R. L., Adamczak, D., Gaitonde, D., Rougeux, A., and Hayes, J., "HIFiRE-1 Boundary Layer Transition Experiment Design," AIAA Paper 2007-534, Jan. 2007.

[12] Wadhams, T. P., Mundy, E., MacLean, M. G., and Holden, M. S., "Ground Test Studies of the HIFIRE-1 Transition Experiment Part I: Experimental Results," *Journal of Spacecraft and Rockets*, Vol. 45, No. 6, 2008, pp. 1134–1148. doi:10.2514/1.38338

[13] Berger, K. T., Greene, F. A., Kimmel, R. L., Alba, C., and Johnson, H., "Aerothermodynamic Testing and Boundary-Layer Trip Sizing of the HIFiRE Flight 1 Vehicle," *Journal of Spacecraft and Rockets*, Vol. 45, No. 6, 2008, pp. 1117–1124. doi:10.2514/1.38722

[14] Keyes, F. G., "A Summary of Viscosity and Heat-Conduction Data for He, A, H_2, O_2, N_2, CO, CO_2, H_2O, and Air," *Transactions of the ASME*, Vol. 73, July 1951, pp. 589–596.

[15] Schneider, S. P., "The Development of Hypersonic Quiet Tunnels," *Journal of Spacecraft and Rockets*, Vol. 45, No. 4, 2008, pp. 641–664. doi:10.2514/1.34489

[16] Liu, T., Cai, Z., Lai, J., Rubal, J., and Sullivan, J. P., "Analytical Method for Determining Heat Flux from Temperature-Sensitive-Paint Measurements in Hypersonic Tunnels," *Journal of Thermophysics and Heat Transfer*, Vol. 24, No. 1, 2010, pp. 85–94. doi:10.2514/1.43372

[17] Casper, K. M., Wheaton, B. M., Johnson, H. B., and Schneider, S. P., "Effect of Freestream Noise on Roughness-Induced Transition at Mach 6," AIAA Paper 2008-4291, June 2008.

[18] Johnson, H. B., and Candler, G. V., "Hypersonic Boundary Layer Stability Analysis Using PSE-Chem," AIAA Paper 2005-5023, June 2005.

[19] Wright, M. J., Candler, G. V., and Bose, D., "A Data-Parallel Line-Relaxation Method for the Navier–Stokes Equations," AIAA Paper 97-2046CP, June 1997.

[20] Nompelis, I., Drayna, T. W., and Candler, G. V., "A Parallel Unstructured Implicit Solver for Hypersonic Reacting Flow Simulation," AIAA Paper 2005-4867, June 2005.

[21] Swanson, E. O., and Schneider, S. P., "Boundary-Layer Transition on Cones at Angle of Attack in a Mach-6 Quiet Tunnel," AIAA Paper 2010-1062, Jan. 2010.

[22] Berry, S. A., and Horvath, T. J., "Discrete-Roughness Transition for Hypersonic Flight Vehicles," *Journal of Spacecraft and Rockets*, Vol. 45, No. 2, March–April 2008, pp. 216–227. doi:10.2514/1.30970

[23] Whitehead, A. H. Jr., "Flowfield and Drag Characteristics of Several Boundary-Layer Tripping Elements in Hypersonic Flow," NASA, TN-D-5454, Oct. 1969.

[24] Danehy, P. M., Ivey, C. B., Inman, J. A., Bathel, B. F., Jones, S. B., McCrea, A. C., Jiang, N., Webster, M., Lempert, W., Miller, J., and Meyer, T., "High-Speed PLIF Imaging of Hypersonic Transition over Discrete Cylindrical Roughness," AIAA Paper 2010-703, Jan. 2010.

R. Kimmel
Associate Editor